was a primary consideration in our choice of a small laboratory angle for measurement.

ACKNOWLEDGMENTS

The authors wish to thank D. D. Yovanovitch, L. G. Ratner, J. G. Asbury, Y. Cho, and T. A. Romanowski for illuminating discussions, and E. Smith for technical assistance during the measurements. Also, we wish to thank Fred Hornstra for measurements of the profile of the external proton beam.[8] One of us (D.E.L.) gratefully acknowledges Fellowship support during this period by Argonne National Laboratory.

[8] F. Hornstra, Jr. and J. R. Simanton, Nucl. Instr. Methods 68, 138 (1969).

PHYSICAL REVIEW D VOLUME 3, NUMBER 5 1 MARCH 1971

K^+p Elastic Scattering at 2.53, 2.76, and 3.20 GeV/c†

J. WHITMORE,* G. S. ABRAMS,‡ L. EISENSTEIN, J. KIM, T. A. O'HALLORAN, JR., AND W. SHUFELDT§
University of Illinois at Urbana-Champaign, Urbana, Illinois 61801
(Received 8 September 1970)

K^+p elastic scattering has been studied at incident kaon momenta of 2.53, 2.76, and 3.20 GeV/c in the Argonne 30-in. hydrogen bubble chamber. Differential cross sections are presented for all scattering angles including the backward direction, where we observe anomalous behavior in the magnitude and slope of the backward peak in this momentum interval. The forward and backward peaks are compared with Regge models and with previously published data. Results are presented of a partial-wave analysis performed at 2.5 GeV/c. While the results are consistent with previous partial-wave analyses at lower energies, the data cannot establish the existence of a resonance in the K^+p system.

I. INTRODUCTION

HERE we report a study of K^+p elastic scattering at 2.53, 2.76, and 3.20 GeV/c. These momenta were selected to study an enhancement in the K^+p total cross section at a c.m. energy of 2505 MeV.[1] The preliminary results of our study of K^+p backward elastic scattering[2] have indicated possible structure in the backward scattering in this momentum region. When combined with the measurements at other momenta,[3–7] our results indicate anomalous behavior in both the shape and magnitude of the backward peak for momenta between 2 and 3 GeV/c. In this paper we present more details of the analysis and our final results. We also compare the data with Regge models based on Λ_α, Λ_γ exchange-degenerate hyperon amplitudes.

In addition we have measured the differential cross section at all angles for K^+p elastic scattering at each of the three momenta. The data are compared with previously reported data in this energy region and confirm the absence of any structure in the differential cross section near $t=-0.8$ (GeV/c)^2, in contrast with K^-p elastic scattering. The data are also found to be in excellent agreement with an extrapolation of the Regge-pole model of Dass *et al.*[8] Using our results at 2.53 GeV/c, we have performed a partial-wave analysis. We are able to conclude that our solutions are in general qualitative agreement with continuations of solutions from previous analyses at lower energies, and find that the data do not demand a K^+p resonance in any partial wave.

II. EXPERIMENTAL PROCEDURE

A. Data Acquisition

The Argonne National Laboratory 30-in. MURA hydrogen bubble chamber was exposed to the ZGS

† Work supported in part by the U. S. Atomic Energy Commission.
* Present address: Argonne National Laboratory, Argonne, Ill.
‡ Present address: Lawrence Radiation Laboratory, University of California, Berkeley, Calif. 94720.
§ Present address: University of Wisconsin at Green Bay, Green Bay, Wisc.

[1] R. J. Abrams, R. L. Cool, G. Giacomelli, T. F. Kycia, B. A. Leontić, K. K. Li, and D. N. Michael, Phys. Rev. Letters 19, 259 (1967).

[2] G. S. Abrams, L. Eisenstein, T. A. O'Halloran, Jr., W. Shufeldt, and J. Whitmore, Phys. Rev. Letters 21, 1407 (1968); G. S. Abrams, L. Eisenstein, J. Kim, T. O'Halloran, Jr., W. Shufeldt, and J. Whitmore, University of Illinois Report No. COO-1195-156, 1969 (unpublished); J. Whitmore, Ph.D. thesis, University of Illinois, 1970 (unpublished).

[3] A. S. Carroll, J. Fischer, A. Lundby, R. H. Phillips, C. L. Wang, F. Lobkowicz, A. C. Melissinos, Y. Nagashima, C. A. Smith, and S. Tewksbury, Phys. Rev. Letters 21, 1282 (1968). We would like to thank Dr. S. Tewksbury for supplying tabulated values of their K^+p backward elastic-scattering data.

[4] P. K. Caldwell, T. Bowen, F. Ned Dikmen, E. W. Jenkins, R. M. Kalbach, D. V. Petersen, and A. E. Pifer, Phys. Rev. D 2, 1 (1970).

[5] J. Banaigs, J. Berger, C. Bonnel, J. Duflo, L. Goldzahl, F. Plouin, W. F. Baker, P. J. Carlson, V. Chabaud, and A. Lundby, Phys. Letters 24B, 317 (1967); Nucl. Phys. B9, 640 (1969).

[6] D. Cline, C. Moore, and D. Reeder, Phys. Rev. Letters 19, 675 (1967).

[7] W. F. Baker, K. Berkelman, P. J. Carlson, G. P. Fisher, P. Fleury, D. Hartill, R. Kalbach, A. Lundby, S. Mukhin, R. Nierhaus, K. P. Pretzl, and J. Woulds, Phys. Letters 29B, 291 (1968).

[8] G. V. Dass, C. Michael, and R. J. N. Phillips, Nucl. Phys. B9, 549 (1969).

TABLE I. Summary of scanning results.

Momentum (GeV/c)		2.53	2.76	3.20
Total two-prong events found		26 000	40 000	41 000
Backward elastic candidates		831	1200	1164
Scanning efficiency for backward elastic candidates		0.92±0.03	0.92±0.02	0.99±0.02
No. of events in the forward sample		9695	3193	2828
Scanning efficiency for forward elastic scatters		0.99±0.01	0.99±0.01	0.99±0.01
Number of three-prong events in each fiducial volume	Backward	1401±39	2167±59	2017±46
	Forward	550±23	164±13	123±11
Three-prong scanning efficiency	Backward	0.95±0.03	0.93±0.02	0.98±0.02
	Forward	0.97±0.01	0.97±0.01	0.99±0.01

high-energy electrostatically separated 7° beam at momenta of 2.53, 2.76, and 3.20 GeV/c. The determination of the beam momenta and the beam contamination have been discussed in a previous publication.[9]

The entire exposure was scanned for all interactions or decays with two or more outgoing particles. The scanning efficiencies were determined by scanning a significant fraction of the film a second time.

The backward scattering cross section is approximately two orders of magnitude lower than the forward scattering cross section. To obtain adequate statistics in the backward direction without measuring all the events, the two-prong events were checked with a template in order to obtain all possible candidates for backward elastic scattering. In addition, a subsample of all the two-prongs found in the scan was measured. In order to facilitate discussion, the two-prongs in the subsample of the film will be called the "forward" sample and those found in the template scan will be called the "backward" sample.

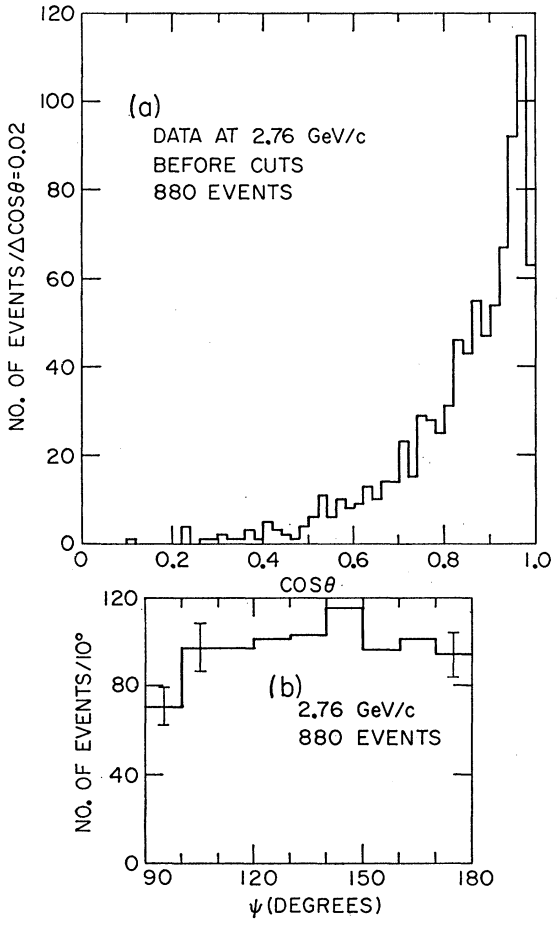

FIG. 1. Distributions of cosθ and bias angle ψ for forward sample at 2.76 GeV/c.

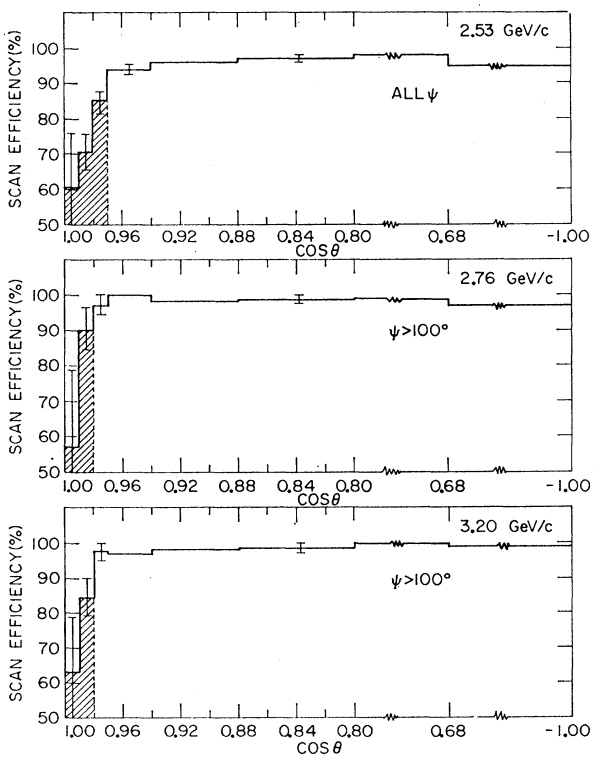

FIG. 2. Single-scan efficiency as a function of cosθ. The shaded areas represent the cutoffs applied in order to obtain an unbiased data sample.

[9] G. S. Abrams, L. Eisenstein, J. Kim, D. Marshall, T. A. O'Halloran, Jr., W. Shufeldt, and J. Whitmore, Phys. Rev. D 1, 2433 (1970).

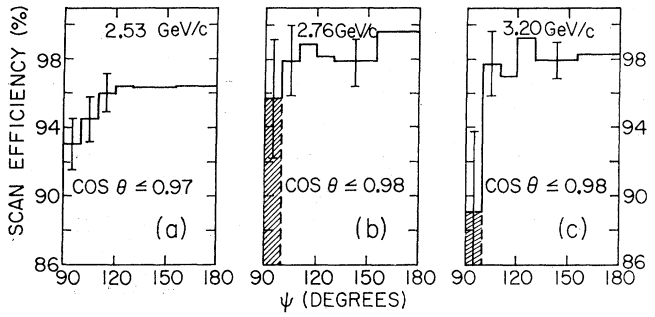

FIG. 3. Single-scan efficiency as a function of bias angle ψ.

To be considered a candidate for the backward sample an event had to satisfy four criteria: (a) The backward track had to make an angle greater than 85° with respect to the beam track; (b) if the backward track stopped, it had to decay; (c) the outgoing tracks could not be on the same side of the beam track; and (d) the forward track had to have a curvature corresponding to a momentum greater than 1.8 GeV/c. The first two conditions were imposed in order to select events having a kaon c.m. scattering angle (θ) satisfying $\cos\theta \leq -0.84$, while the last two were an attempt to eliminate inelastic events.

A summary of the scanning results for the two-prong topology is given in Table I. Also shown in Table I are the numbers of beam-associated τ-like decays at each momentum that satisfy the same fiducial volume and beam track criteria as the selected two-prong events. These three-prong events were used to normalize the beam flux in the backward and forward fiducial volumes.

B. Event Processing

The two-prong events were measured (in three views) on scanning and measuring projectors (SMP's). Reconstruction and kinematic fitting of the events were performed using standard University of Illinois programs. Remeasurements were made at all three energies on the backward candidates and at 2.53 and 2.76 GeV/c on the forward sample. A comparison of the failing events from the first measurement pass at 3.20 GeV/c with those at 2.76 GeV/c suggested no significant biases in the remeasurement sample and no remeasurement pass was performed at 3.20 GeV/c. The cross sections at this highest momentum have therefore been corrected for event reconstruction losses on the basis of the 2.76-GeV/c data.

A large fraction of the elastic scatters also fit other hypotheses. The forward elastic events, with $\cos\theta \gtrsim 0.7$, were generally ambiguous with a four-constraint (4C) fit to the hypothesis $\pi^+p \rightarrow \pi^+p$ and/or a one-constraint (1C) fit to the $K^+p \rightarrow K^+p\pi^0$ hypothesis under an interchange of charged tracks. A study of the pion contamination at 3.20 GeV/c [10] indicates that the beam contamination by pions is $(0.7\pm0.2)\%$. After correcting for the difference between the π^+p and K^+p elastic cross sections, we estimate that fewer than 2% of the elastic events at 3.20 GeV/c are due to π^+p elastic scattering.

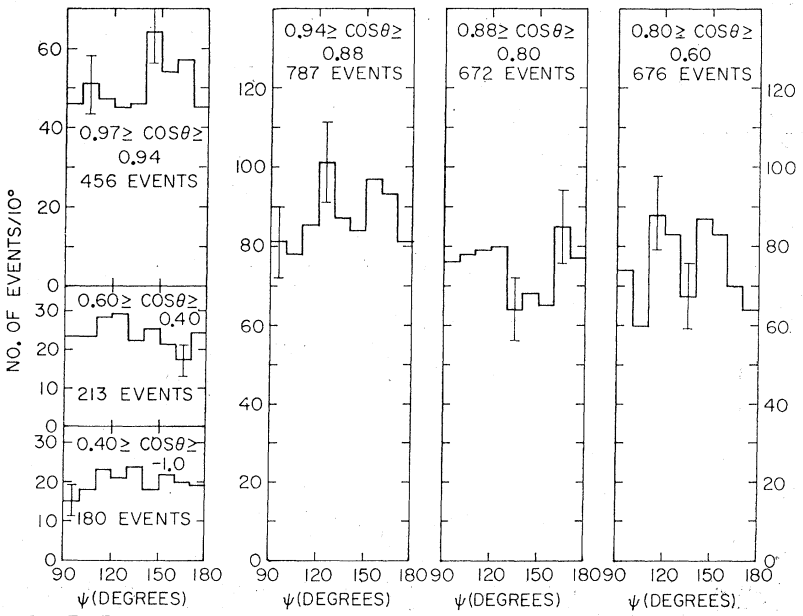

FIG. 4. Distribution of bias angle for different $\cos\theta$ regions at 2.53 GeV/c.

[10] L. Eisenstein, University of Illinois Physics Department Technical Report No. 177, 1969 (unpublished).

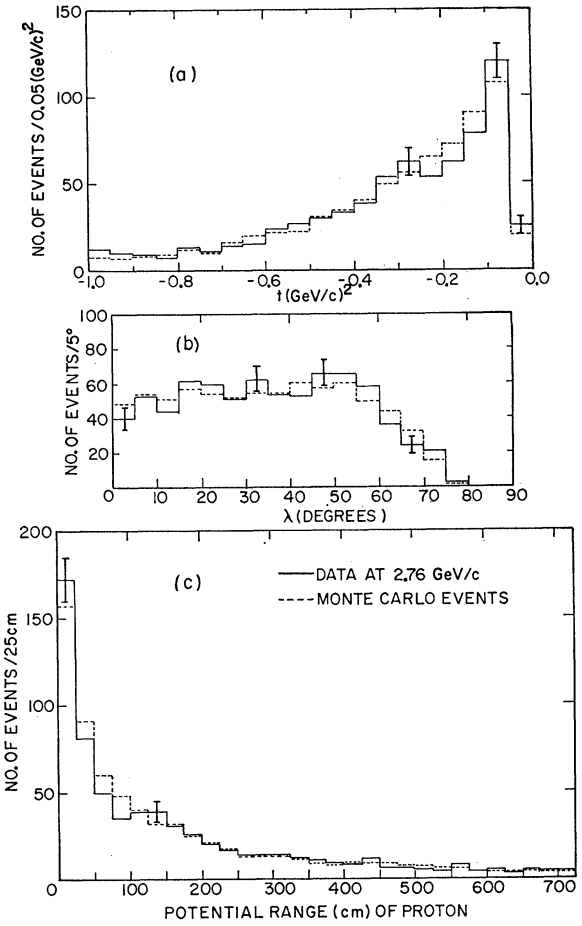

FIG. 5. Comparison between the data at 2.76 GeV/c (solid lines) and a Monte Carlo calculation (dashed lines). (a) Momentum transfer squared; (b) proton dip angle λ; (c) proton potential range.

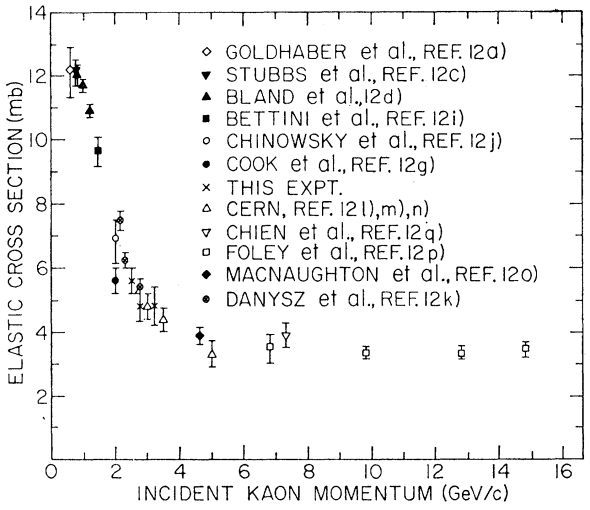

FIG. 6. Elastic cross section as a function of incident K^+ momentum.

During the entire run, the light-particle contamination was monitored with a Cherenkov counter in the beam which indicated that the pion contamination at the other momenta was consistent with that observed at 3.20 GeV/c. A visual examination of a sample of events with a 4C-1C ambiguity under an interchange of charged tracks indicated that the observed bubble densities were normally inconsistent with the 1C fit and confirmed the 4C hypothesis. On the basis of the above studies, the 4C K^+ incident hypothesis was selected for final analysis.

The backward elastic events with $\cos\theta \leq -0.8$ were usually kinematically ambiguous with a fit to the reaction $\pi^+p \rightarrow \pi^+p\pi^0$, with the neutral pion having a momentum of less than 200 MeV/c. This ambiguity was resolved on the basis of the observed ionization.

C. Bias Studies

To look for scanning biases in the backward elastic scattering data, the distribution of the scattering plane about the beam direction was studied at each momentum. With ψ defined by the expression $\cos\psi = \hat{n}\cdot\hat{z}$, where $\hat{n}$ is a unit vector normal to the scattering plane and $\hat{z}$ is a unit vector normal to the chamber window, a small depletion in the observed number of events for $90° \leq \psi \leq 120°$ was found at 2.76 GeV/c.[2] These events were lost in a systematic manner by the template scan. The bias, which was only apparent for forward tracks on one side of the beam track direction, arises from the curvature of the beam. When the forward track is within 2° of the beam track the scanner considers both outgoing tracks to be on the same side of the beam track and therefore considers the event to be inelastic. This bias was easily corrected by discarding events within the 2° on the biased side and repopulating, using events on the unbiased side. The corrections are small and do not affect any of the conclusions to be drawn later. The template scanning criteria were subsequently modified at 2.53 and 3.20 GeV/c and events with a backward track were not rejected if the forward track lay within

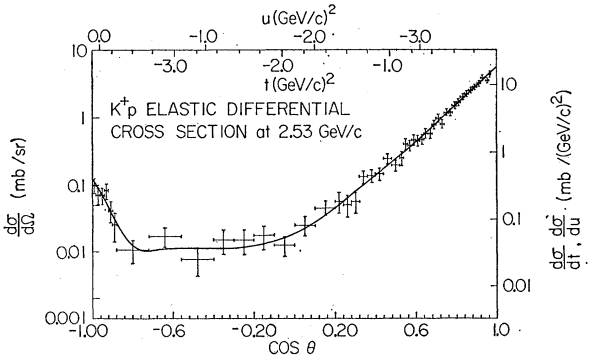

FIG. 7. Differential cross section for K^+p elastic scattering at 2.53 GeV/c. The curves are the results of the best fit to a Legendre polynomial expansion.

TABLE II. Summary of cross sections.

Momentum (GeV/c)		2.53	2.76	3.20
Statistical level of study (ev/μb)	Backward	1.68±0.09	2.90±0.18	2.97±0.18
	Forward	0.64±0.04	0.21±0.02	0.18±0.02
Total elastic cross sections (mb)		5.60±0.40	4.75±0.49	4.81±0.63

2° on either side of the beam direction. The resulting ψ distributions obtained at 2.53 and 3.20 GeV/c were consistent with isotropy and no corrections were necessary.

An additional systematic loss of events in the forward direction ($\cos\theta\simeq 1$) was observed. This is a combination of a scanning loss of short-length proton tracks and a scanning loss due to the orientation of the scattering plane. These losses are illustrated in Fig. 1, which shows the $\cos\theta$ and bias angle ψ distributions at 2.76 GeV/c. There is a loss of events near $\psi=90°$, indicating a preference for events with their scattering plane parallel to the front glass of the chamber.

To correct for these losses, the scanning efficiency has been studied as a function of $\cos\theta$ and the results are shown in Fig. 2. The efficiencies at 2.76 and 3.20 GeV/c have been calculated for events with $\psi\geq 100°$ on the basis of Fig. 3, which presents the scanning efficiency as a function of ψ. While the need for a cutoff of $\psi\geq 100°$ at 2.76 GeV/c would appear to be marginal in Fig. 3(b), it was decided that this cut should be made on the basis of the preferential loss of events near $\psi=90°$ [Fig. 1(b)]. The data therefore indicate that unbiased data samples may be obtained at 2.76 and 3.20 GeV/c if we require that $\cos\theta\leq 0.98$ and $\psi\geq 100°$. After studying the distributions at 2.53 GeV/c (Fig. 4) we find that only a $\cos\theta\leq 0.97$ cut was required. No evidence for a significant bias as a function of ψ could be found for any region in $\cos\theta$.

To determine whether the resulting distributions, after the angular cuts had been made, were consistent with the distributions expected for elastic scattering, a comparison was then made at 2.76 GeV/c between the data and some Monte-Carlo-generated events. 10 000 events were generated, assuming (a) elastic scattering, (b) an exponential t (defined as the four-momentum transfer squared between initial and final kaon) distribution with slope 3.10 (GeV/c)$^{-2}$ (as observed at 2.76 GeV/c), and (c) an isotropic distribution in ψ. The angular restrictions $\cos\theta\leq 0.98$ and $\psi\geq 100°$ were then imposed and the results normalized to the number of events at 2.76 GeV/c. The distributions that were compared, the momentum transfer distribution, the potential range of the proton (as calculated from the fitted momentum), and the dip angle λ are shown in Fig. 5. The solid lines indicate data, and the dashed lines indicate the Monte Carlo events. The close agreement between the experimental and Monte-Carlo-generated data confirms that the above cuts did indeed effect an unbiased sample of events.

The cross sections to be presented in Sec. II D have been determined from the number of elastic events, corrected for both $\cos\theta$ and ψ cutoffs and for the over-all scanning efficiency based on the events within the above angular cutoff limits. The efficiencies used are tabulated in Table I.

D. Cross Sections

The cross sections presented in this paper have been determined by normalizing the number of elastic scatters within a fiducial volume to the number of three-prong events found in that same volume. Using a τ-like decay branching ratio of 0.060±0.001,[11] the statistical levels and elastic cross sections found in this experiment

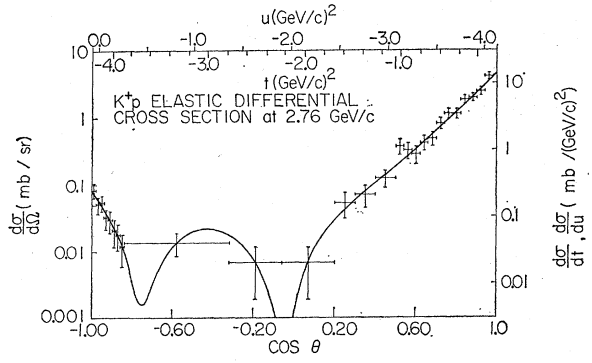

FIG. 8. Differential cross section for K^+p elastic scattering at 2.76 GeV/c. The curves are the results of the best fit to a Legendre polynomial expansion.

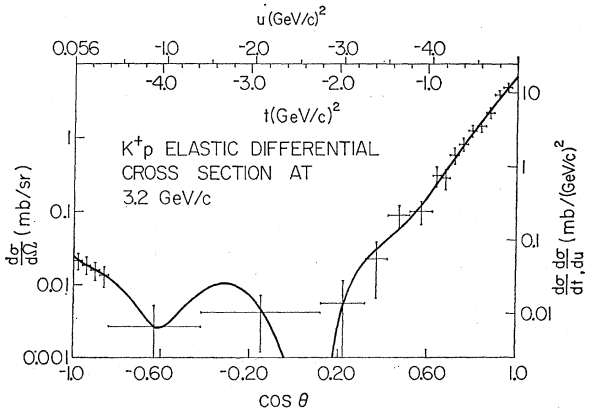

FIG. 9. Differential cross section for K^+p elastic scattering at 3.20 GeV/c. The curves are the results of the best fit to a Legendre polynomial expansion.

[11] G. Trilling, LRL Report No. UCRL-16473, 1965 (unpublished).

are shown in Table II. The total elastic cross sections were determined to be 5.60±0.40, 4.75±0.49, and 4.81±0.63 mb at 2.53, 2.76, and 3.20 GeV/c, respectively. The elastic cross sections have been corrected for the cosθ region near 1.0 by an exponential extrapolation and are compared with previously reported data[12] in Fig. 6.

The differential cross sections obtained in this experiment are presented in Table III. The observed numbers of events reported in Table III are the numbers that remain after the various cosθ and ψ cuts have been made (see Sec. II C). The characteristic features of the distributions shown in Figs. 7–9 are (1) a dominant diffraction peak in the region $|t|<2$ (GeV/c)^2, (2) no evidence for any structure near $|t|=0.8$ (GeV/c)^2, and (3) a significant backward peak.

III. ANALYSIS OF BACKWARD ELASTIC SCATTERING

A. Differential Cross Sections

Recently K^+p elastic scattering in the backward direction has been studied extensively between laboratory momenta of 0.41 and 6.9 GeV/c. Below 1 GeV/c the interaction is dominated by S-wave scattering and the backward differential cross section has an essentially constant value of about 0.9 mb/sr.[4,13] Above 1 GeV/c,[3] the 180° cross section begins to drop rapidly, and at momenta above 1.4 GeV/c, the angular distribution is characterized by the onset of a backward peak. Published data presently exist below 2.45 GeV/c,[3] and at 3.55,[5,6] 5.2, and 6.9 GeV/c.[7] In this paper we present backward cross sections at 2.53, 2.76, and 3.20 GeV/c.

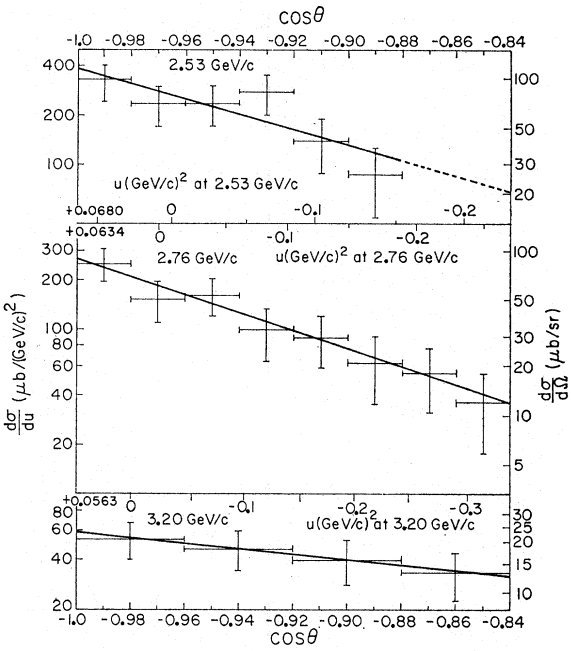

FIG. 10. Backward differential cross sections as a function of cosθ. The curves are the results of the best fit to the form $d\sigma/du = Ae^{Bu}$, as described in the text.

Shown in Fig. 10 are the cross sections from this experiment as a function of cosθ for cos$\theta \leq -0.84$. The most apparent feature is the difference both in shape and magnitude between the 3.20-GeV/c data and the data at the two lower energies.[14] In order to study this difference in a more quantitative manner, we parametrize the distributions by the forms

$$\frac{d\sigma}{d\Omega} = \frac{d\sigma}{d\Omega}(180°)e^{A(1+\cos\theta)}$$

and

$$\frac{d\sigma}{du} = \frac{d\sigma}{du}(u=0)e^{Bu},$$

where u is the four-momentum transfer squared between the incident kaon and outgoing proton.

[12] K^+p elastic scattering: (a) 0.140–0.642 GeV/c—S. Goldhaber, W. Chinowsky, G. Goldhaber, W. Lee, T. O'Halloran, T. F. Stubbs, G. M. Pjerrou, D. H. Stork, and H. K. Ticho, Phys. Rev. Letters **9**, 135 (1962); (b) 0.780 GeV/c—S. Focardi, A. Minguzzi-Ranzi, L. Monari, G. Saltini, P. Serra, T. A. Filippas, and V. P. Henri, Phys. Letters **24B**, 314 (1967); (c) 0.810 GeV/c—T. F. Stubbs, H. Bradner, W. Chinowsky, G. Goldhaber, S. Goldhaber, W. Slater, D. M. Stork, and H. K. Ticho, Phys. Rev. Letters **7**, 188 (1961); (d) 0.864, 0.969, and 1.207 GeV/c—R. W. Bland, G. Goldhaber, and G. H. Trilling, Phys. Letters **29B**, 618 (1969); (e) 0.864–1.585 GeV/c—R. W. Bland, M. G. Bowler, J. L. Brown, J. A. Kadyk, G. Goldhaber, S. Goldhaber, V. H. Seeger, and G. H. Trilling, Nucl. Phys. **B13**, 595 (1969); (f) 0.910 GeV/c—W. Hirsch and G. Gidal, Phys. Rev. **135B** 191 (1964); (g) 0.970, 1.170, and 1.970 GeV/c—V. Cook, D. Keefe, L. T. Kerth, P. G. Murphy, W. A. Wenzel, and T. F. Zipf, *ibid.* **129**, 2743 (1963); (h) 1.207, 1.365, and 1.96 GeV/c—R. W. Bland, G. Goldhaber, B. H. Hall, J. A. Kadyk, V. H. Seeger, G. H. Trilling, and C. G. Wohl, LRL Report No. UCRL-18323, 1968 (unpublished); (i) 1.45 GeV/c—A. Bettini, M. Cresti, S. Limentani, L. Peruzzo, R. Santangelo, D. Locke, D. J. Crennell, W. T. Davies, and P.B . Jones, Phys. Letters **16**, 83 (1965); (j) 1.96 GeV/c—W. Chinowsky, G. Goldhaber, S. Goldhaber, T. O'Halloran, and B. Schwarzschild, Phys. Rev. **139**, B1411 (1965); (k) 2.11, 2.31, 2.53, and 2.72 GeV/c—J. A. Danysz, M. Spiro, A. Verglas, J. M. Brunet, J. L. Narjoux, B. Penney, G. Thompson, P. H. Lewis, J. E. Allen, and P. V. March, Nucl. Phys. **B14**, 161 (1969); (l) 2.97 GeV/c—J. Debaisieux, F. Grard, J. Heughebaert, L. Pape, R. Windmolders, R. George, Y. Goldschmidt-Clermont, V. P. Henri, D. W. G. Leith, G. R. Lynch, F. Muller, J.-M. Perreau, G. Otter, and P. Sällström, Nuovo Cimento **43A**, 142 (1966); (m) 2.97, 3.46, and 4.97 GeV/c—Y. Goldschmidt-Clermont, V. P. Henri, B. Jongejans, A. Moisseev, F. Muller, J.-M. Perreau, A. Prokes, V. Yarba, W. De Baere, J. Debaisieux, P. Dufour, F. Grard, J. Heughebaert, L. Pape, P. Peeters, F. Verbeure, and R. Windmolders, *ibid.* **46A**, 539 (1966); (n) 3.46 and 4.97 GeV/c—W. De Baere, J. Debaisieux, P. Dufour, F. Grard, J. Heughebaert, L. Pape, P. Peeters, F. Verbeure, R. Windmolders, R. George, Y. Goldschmidt-Clermont, V. P. Henri, B. Jongejans, D. W. G. Leith, A. Moisseev, F. Muller, J.-M. Perreau, and V. Yarba, *ibid.* **45A**, 885 (1966); (o) 4.6 GeV/c—J. N. MacNaughton, L. Feinstein, F. Marcelja, and G. H. Trilling, Nucl. Phys. **B14**, 237 (1969); (p) 6.8, 9.8, 12.8, and 14.8 GeV/c—K. J. Foley, S. J. Lindenbaum, W. A. Love, S. Ozaki, J. J. Russell, and L. C. L. Yuan, Phys. Rev. Letters **11**, 503 (1963); (q) 7.3 GeV/c—C.-Y. Chien, E. Malamud, D. J. Mellema, P. E. Schlein, W. E. Slater, D. H. Stork, and H. K. Ticho, Phys. Letters **28B**, 615 (1969).

[13] See S. Goldhaber *et al.*, Ref. 12(a).

[14] Because of this difference, we rescanned the entire film at 3.20 GeV/c looking for additional candidates for backward elastic scatters. No new candidates were found and we are confident that at this energy the template scan was almost 100% efficient.

TABLE III. Experimental angular distributions.

Interval in cosθ	Observed no. events	$\frac{d\sigma}{d\Omega}$ (mb/sr)	Interval in cosθ	Observed no. events	$\frac{d\sigma}{d\Omega}$ (mb/sr)
		at 2.53 GeV/c			
1.00	Extrapolated	5.48 ±0.29	0.48, 0.44	39	0.24 ±0.04
0.97, 0.96	173	4.29 ±0.44	0.44, 0.40	23	0.14 ±0.03
0.96, 0.94	283	3.51 ±0.32	0.40, 0.36	22	0.14 ±0.03
0.94, 0.92	308	3.82 ±0.34	0.36, 0.32	21	0.13 ±0.03
0.92, 0.90	255	3.16 ±0.29	0.32, 0.28	9	0.056±0.019
0.90, 0.88	224	2.78 ±0.27	0.28, 0.24	8	0.050±0.018
0.88, 0.86	201	2.49 ±0.25	0.24, 0.20	9	0.056±0.019
0.86, 0.84	178	2.21 ±0.22	0.20, 0.10	18	0.045±0.011
0.84, 0.82	160	1.98 ±0.21	0.10, 0.00	10	0.025±0.008
0.82, 0.80	133	1.65 ±0.18	0.00, −0.10	5	0.012±0.004
0.80, 0.78	120	1.49 ±0.17	−0.10, −0.20	7	0.017±0.007
0.78, 0.76	94	1.17 ±0.14	−0.20, −0.30	6	0.015±0.006
0.76, 0.74	93	1.15 ±0.14	−0.30, −0.40	6	0.015±0.006
0.74, 0.72	63	0.78 ±0.11	−0.40, −0.56	5	0.008±0.004
0.72, 0.70	78	0.97 ±0.13	−0.56, −0.72	11	0.017±0.005
0.70, 0.68	62	0.77 ±0.11	−0.72. −0.88	8	0.011±0.004
0.68, 0.66	46	0.57 ±0.09	−0.88, −0.90	5	0.026±0.012
0.66, 0.64	46	0.57 ±0.09	−0.90, −0.92	8	0.042±0.015
0.64, 0.62	38	0.47 ±0.08	−0.92, −0.94	16	0.083±0.021
0.62, 0.60	36	0.45 ±0.08	−0.94, −0.96	14	0.071±0.019
0.60, 0.58	37	0.46 ±0.08	−0.96, −0.98	14	0.071±0.019
0.58, 0.56	31	0.38 ±0.07	−0.98, −1.00	19	0.099±0.024
0.56, 0.54	32	0.40 ±0.08	−1.00	Extrapolated	0.110±0.030
0.54, 0.52	20	0.25 ±0.06			
0.52, 0.48	31	0.19 ±0.04		Total 3035	
		at 2.76 GeV/c			
1.00	Extrapolated	4.77 ±0.34	0.40, 0.30	8	0.071±0.026
0.98, 0.94	188	4.16 ±0.50	0.30, 0.20	6	0.053±0.022
0.94, 0.90	114	2.52 ±0.34	0.20, −0.06	2	0.007±0.005
0.90, 0.86	91	2.02 ±0.29	−0.06, −0.32	2	0.007±0.005
0.86, 0.82	84	1.86 ±0.27	−0.32, −0.84	8	0.014±0.005
0.82, 0.78	52	1.15 ±0.19	−0.84, −0.86	4	0.012±0.006
0.78, 0.74	52	1.15 ±0.19	−0.86, −0.88	6	0.018±0.008
0.74, 0.70	37	0.82 ±0.16	−0.88, −0.90	6	0.021±0.009
0.70, 0.66	22	0.49 ±0.11	−0.90, −0.92	9	0.030±0.011
0.66, 0.62	19	0.42 ±0.11	−0.92, −0.94	11	0.033±0.012
0.62, 0.58	13	0.29 ±0.09	−0.94, −0.96	17	0.054±0.014
0.58, 0.54	15	0.33 ±0.09	−0.96, −0.98	17	0.051±0.014
0.54, 0.50	17	0.38 ±0.10	−0.98, −1.00	26	0.084±0.019
0.50, 0.40	14	0.12 ±0.04	−1.00	Extrapolated	0.089±0.019
				Total 840	
		at 3.20 GeV/c			
1.00	Extrapolated	7.01 ±0.63	0.52, 0.42	8	0.089±0.033
0.98, 0.94	169	4.72 ±0.65	0.42, 0.32	2	0.022±0.016
0.94, 0.90	135	3.77 ±0.54	0.32, 0.12	1	0.006±0.006
0.90, 0.86	76	2.12 ±0.34	0.12, −0.42	2	0.004±0.003
0.86, 0.82	51	1.42 ±0.26	−0.42, −0.84	1	0.003±0.003
0.82, 0.78	44	1.23 ±0.23	−0.84, −0.88	10	0.014±0.004
0.78, 0.74	29	0.81 ±0.18	−0.88, −0.92	12	0.016±0.005
0.74, 0.70	21	0.59 ±0.15	−0.92, −0.96	14	0.019±0.005
0.70, 0.66	10	0.28 ±0.09	−0.96, −1.00	16	0.022±0.006
0.66, 0.62	11	0.31 ±0.10	−1.00	Extrapolated	0.023±0.009
0.62, 0.52	9	0.100±0.035		Total 621	

The results of this analysis are given in Table IV and shown as the curves in Fig. 10. In Figs. 11 and 12 we present a comparison of our data with those of previously published experiments.[3,5–7] It is apparent that in the momentum interval 2–3 GeV/c both the differential cross section at 180° (Fig. 11) and the slope of the backward peak (Fig. 12) deviate from a monotonic energy dependence.

TABLE IV. Results of a two-parameter fit to backward peak.

Momentum (GeV/c)	Maximum cosθ	$\frac{d\sigma}{d\Omega}(180°)$ (μb/sr)	B (GeV/c)$^{-2}$
2.53	−0.88	112±26	5.7±2.0
2.76	−0.84	89±19	6.1±1.4
3.20	−0.84	23±9	1.6±1.8

We note that our results are in good agreement with those at nearby energies. Our results at the two lower momenta agree both in shape and normalization with the data of Carroll *et al.*[3] at 2.20, 2.33, and 2.45 GeV/c and our 3.20-GeV/c data are consistent with the results

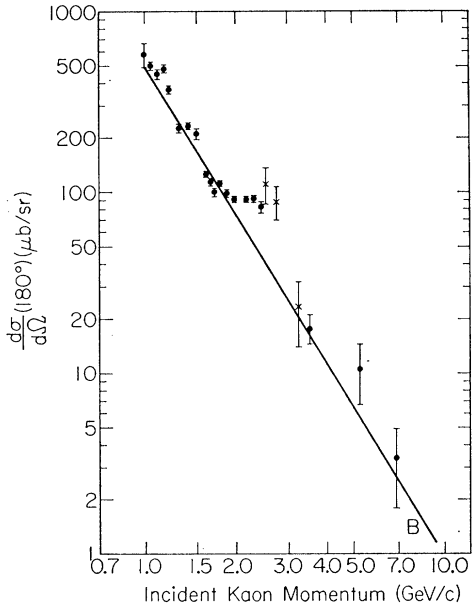

FIG. 11. The variation of the backward differential cross section $d\sigma/d\Omega(180°)$ as a function of incident kaon momentum. The curve is the result of the fit described in the text.

of Banaigs *et al.*[5] and Cline *et al.*[6] at 3.5 GeV/c. This is in contrast to the recently published result at 1.20 GeV/c in which the bubble-chamber data of Bland *et al.*[15] disagree in normalization with the counter measurements of Carroll *et al.*[3] It should be noted that the shoulder observed in the differential cross section at 180° between 2 and 3 GeV/c is not as apparent if one plots the cross section at $u=0$, as has been done previously. The 180° cross section is approximately constant between 2 and 3 GeV/c, but the slope of the backward peak varies by a factor of ~ 3. As a result, the $u=0$ cross section decreases as a function of energy in this momentum interval.

B. Discussion of Results

Barger has noted that since the K^+p elastic amplitude has no direct-channel resonances one would expect Reggeized baryon exchange to account for the K^+p backward peak to rather low momentum.[16] We note that the absence of any dip or levelling off in the K^+p elastic differential cross section at 180° indicates that there is no single trajectory dominating this process.[17]

[15] See R. W. Bland *et al.*, Ref. 12(d). There appear to be systematic discrepancies between the experiments. While the cross sections determined by Bland *et al.* are larger than the cross sections of Carroll *et al.* (Ref. 3), the cross sections determined by Bettini *et al.* [Ref. 12(i)] are smaller. All of the experiments give consistent results for the slope of the backward cross section. In the interest of simplicity we have chosen to base our analysis on the data of Carroll *et al.*, which extend into the energy region of our experiment.

[16] V. Barger, Phys. Rev. **179**, 1371 (1969).

[17] The Λ_α amplitude has a signature zero at $\alpha=-\frac{1}{2}$. Figure 13 indicates that this would occur near $u=+0.2$ (GeV/c)^2, which at most energies is outside the physical region. Thus one would expect to see the differential cross section dip or level off near $\cos\theta=-1$ if the Λ_α dominates. Similar arguments hold for the amplitudes from other trajectories.

[18] P. B. James, Phys. Rev. **179**, 1559 (1969).

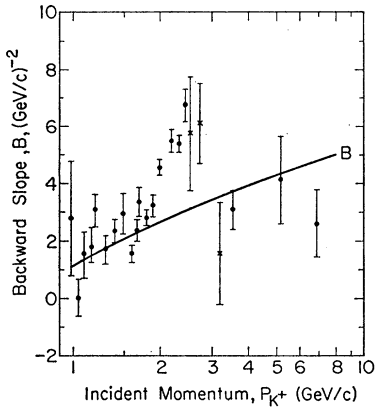

FIG. 12. Slope of the backward peak as a function of incident kaon momentum. The curve is the result of the fit described in the text.

Duality further imposes the requirement that the backward K^+p elastic amplitude be real. In addition, Barger, on the basis of $SU(3)$, the backward peak in the reaction $K^-p \to \Lambda_\gamma(1520)\pi^0$, and the relative isospin contributions to K^-p elastic scattering, asserts that the $I=0$ exchange contributions should be large relative to the $I=1$ terms in the K^+p backward elastic scattering amplitude. We therefore follow the work of James[18]

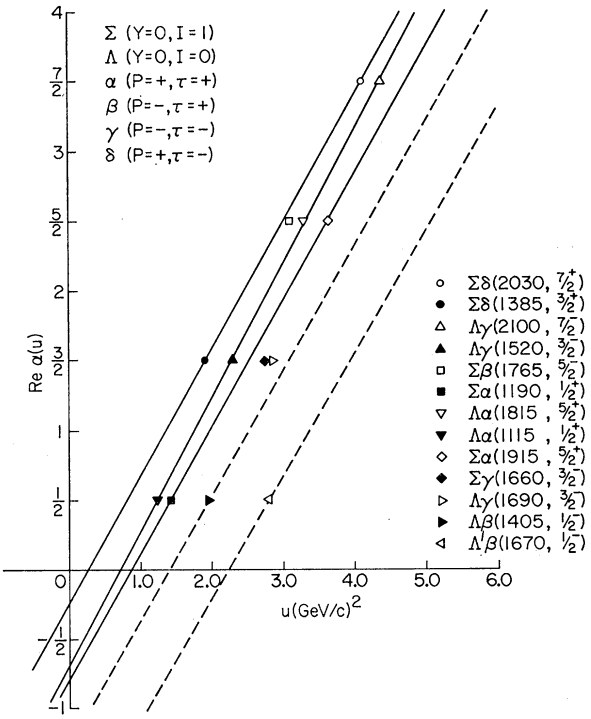

FIG. 13. Chew-Frautschi plot of spin vs mass squared for most of the known hyperons.

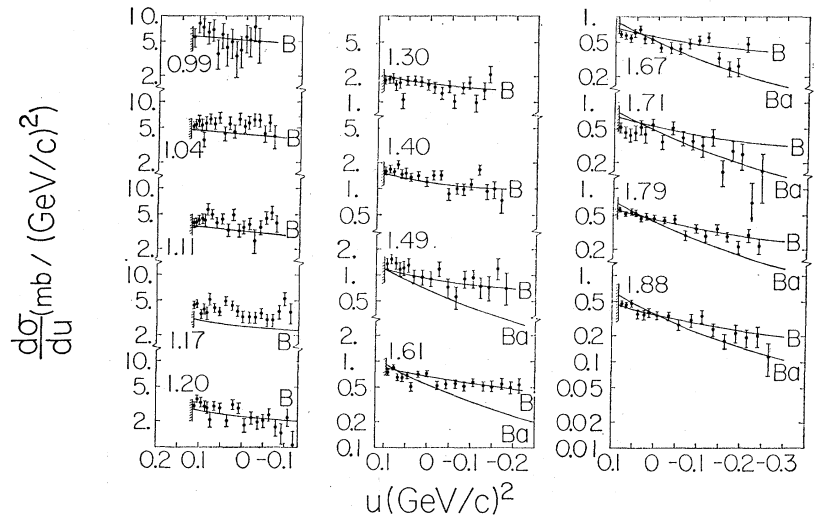

FIG. 14. K^+p backward angular distributions from 0.99 to 1.88 GeV/c. The curves labeled Ba are from Barger (Ref. 16). The curves labeled B are the results of the fit described in the text.

and Barger[16] and use the Λ_α, Λ_γ exchange-degenerate (EXD) pair of trajectories.

Following the notation of Barger and Cline,[19] we write the real u-channel amplitude as

$$f_1(\sqrt{u}, s)=\frac{E_u+m}{\sqrt{u}}\gamma(u)2\frac{\Gamma(\frac{1}{2}-\alpha)}{\pi}\left(\frac{s-m^2-\mu^2}{s_0}\right)^{\alpha-1/2}.$$

The crossing-symmetry relation

$$f_1(\sqrt{s}, u)=\frac{E_s+m}{2\sqrt{s}}\left[(\sqrt{u}-\sqrt{s}+2m)\frac{f_1(\sqrt{u}, s)}{E_u+m}+(\sqrt{u}+\sqrt{s}-2m)\frac{f_1(-\sqrt{u}, s)}{E_u-m}\right]$$

is then used to obtain

$$f_1(\sqrt{s}, u)=\frac{E_s+m}{\sqrt{s}}\frac{2\Gamma(\frac{1}{2}-\alpha)}{\pi}\gamma\left(\frac{s-m^2-\mu^2}{s_0}\right)^{\alpha-1/2}, \quad (1)$$

where s is the square of the total c.m. energy, $E_s=(s+m^2-\mu^2)/2\sqrt{s}$ is the c.m. energy of the proton, m and μ are the proton and kaon masses, γ is an effective residue function taken as a constant, s_0 is a scaling constant, and $\alpha=\alpha(u)$ is the Λ_α, Λ_γ EXD trajectory.

The differential cross section is then given by

$$d\sigma/d\Omega=|f_1(\sqrt{s}, u)|^2+|f_1(-\sqrt{s}, u)|^2-2\cos\theta[f_1(\sqrt{s}, u)f_1(-\sqrt{s}, u)]. \quad (2)$$

A fit to all existing differential cross section data has been performed using Eqs. (1) and (2) with a $(\Lambda_\alpha,\Lambda_\gamma)$ trajectory

$$\alpha(u)=-0.70+0.95u,$$

as obtained from the Chew-Frautschi plot shown in Fig. 13. Because of the anomalous behavior of the data between 2 and 3 GeV/c, these data have been excluded from the fit. The two-parameter fit to the 264 data points yielded the values $s_0=1.01$ GeV^2 and $|\gamma|=3.20$ GeV^{-1} with a resulting $\chi^2=709$. It should be noted that no adjustments of the data have been made and only statistical errors have been used.

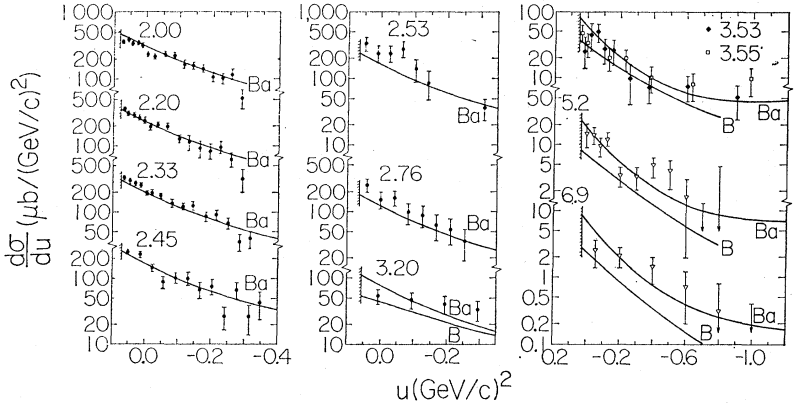

FIG. 15. K^+p backward angular distributions from 2.00 to 6.9 GeV/c. The curves labeled Ba are from Barger (Ref. 16). The curves labeled B are the results of the fit described in the text.

[19] V. Barger and D. Cline, Phys. Rev. **155**, 1792 (1967).

TABLE V. Results of a three-parameter fit to diffraction peak.

Momentum (GeV/c)	t range (GeV/c)^2	B (GeV/c)$^{-2}$	C (GeV/c)$^{-4}$
2.53	−0.06, −0.86	3.1±0.5	−0.4±0.6
	−0.06, −1.16	3.5±0.3	0.1±0.3
2.76	−0.05, −0.70	3.6±1.9	0.6±2.8
	−0.05, −1.20	3.5±1.0	0.4±1.0
3.20	−0.05, −0.70	3.7±1.3	0.2±2.0
	−0.05, −1.00	3.5±1.2	0.2±1.4

In order to find a more satisfactory parametrization of the data, the following amplitude has been used instead of Eq. (1):

$$f_1(\sqrt{s},u)=\frac{E_s+m}{\sqrt{s}}\frac{2}{\pi^{3/2}}\gamma B(1-\alpha_t,\tfrac{1}{2}-\alpha_u), \qquad (3)$$

where $B(x,y)=\Gamma(x)\Gamma(y)/\Gamma(x+y)$ and $\alpha_t=0.5+t$ is the EXD t-channel meson trajectory (ρ,A_2,P',ω). A one-parameter fit to Eq. (3) gave a significantly better fit to the low-momenta data between 1.04 and 1.67 GeV/c and yielded the value $|\gamma|=4.58$ GeV^{-1} with $\chi^2=567$ for 264 data points. This fit is shown in Figs. 11, 12, 14, and 15 as the solid line curves labelled B. It should be noted that large contributions to the values of χ^2 result from entire data sets being high (e.g., 1.17 GeV/c) or low (e.g., 1.71 GeV/c). Whether these deviations are the results of normalization difficulties[15] or have a greater significance is not clear. It is seen, however, that such a simple model does in fact give an adequate parametrization of the data from 1 to 7 GeV/c except for the momentum interval 2–3 GeV/c.

Also shown in Figs. 14 and 15 (as the curves labeled Ba) are the results of a fit by Barger[16] to the data above 2 GeV/c using a u-dependent residue function. While the fit is excellent above 2 GeV/c, it is apparent that one cannot extrapolate such a parametrization below 2 GeV/c.

In conclusion, it seems that a simple hyperon exchange model employing EXD Λ_α, Λ_γ trajectories is able to parametrize adequately the K^+p backward elastic scattering data from 1 to 7 GeV/c, with the notable exception of the 2–3-GeV/c momentum interval.[20] Furthermore, it is interesting to note that this interval coincides with the enhancement at 2.505 GeV in the K^+p total cross section as measured by Abrams *et al.*[1]

TABLE VI. Results of a two-parameter fit to diffraction peak.

Momentum (GeV/c)	t range (GeV/c)^2	No. of events	B (GeV/c)$^{-2}$
2.53	−0.06, −0.71	2514	3.44±0.17
	−0.06, −1.01	2729	3.36±0.12
	−0.06, −1.21	2794	3.32±0.11
	−0.06, −1.71	2861	3.25±0.09
2.76	−0.05, −0.70	610	3.24±0.24
	−0.05, −1.00	672	3.05±0.17
	−0.05, −1.20	687	3.11±0.15
	−0.05, −1.70	705	3.04±0.13
3.20	−0.05, −0.70	513	3.62±0.27
	−0.05, −1.00	547	3.66±0.20
	−0.05, −1.20	555	3.69±0.18
	−0.05, −1.70	565	3.62±0.16

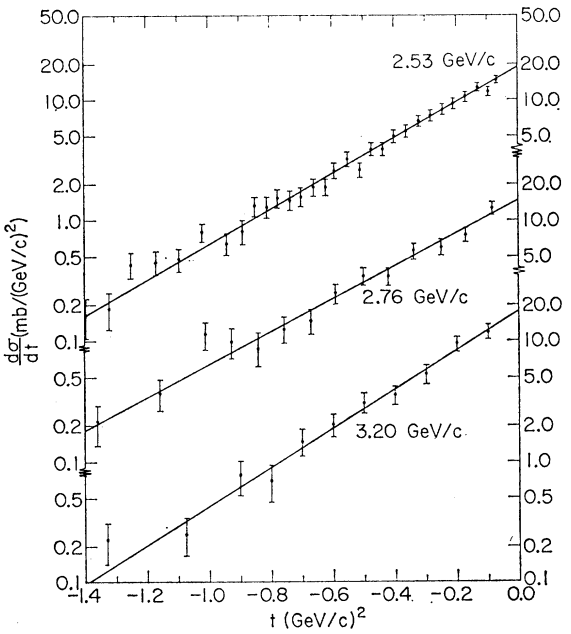

FIG. 16. Forward differential cross sections. The solid line curves are the results of the best fit to the form $d\sigma/dt=Ae^{Bt}$ as described in the text.

IV. ANALYSIS OF FORWARD ELASTIC SCATTERING

A. Forward Differential Cross Sections

The experimental angular distributions (after making corrections for the cosθ and azimuthal cuts) are shown in Fig. 16 as a function of t. We have parametrized the data with the functional form

$$d\sigma/dt=Ae^{Bt+Ct^2}. \qquad (4)$$

The results of a maximum-likelihood fit to the data are given in Table V. Previous analyses of K^+p elastic scattering have indicated the possible need for the quadratic term in Eq. (4).[21] In all of our results, however, the parameter C is consistent with zero. This was also found in an analysis of K^+p elastic scattering at 7.3 GeV/c,[22] and it indicates that the quadratic term is not needed. Table VI gives the results of a two-parameter fit with $C=0$ for four regions of t. The fact that B does not vary significantly as the t range is increased out to −1.70 (GeV/c)^2 is a further indication that a quadratic term is not required for our data. The results of the

[20] E. L. Berger and G. C. Fox, Phys. Rev. **188**, 2120 (1969), after an extensive study using the Veneziano model for KN scattering are also unable to fit this 2–3 GeV/c interval.

[21] See K. J. Foley *et al.*, Ref. 12(p).

[22] See C. Y. Chien *et al.*, Ref. 12(q).

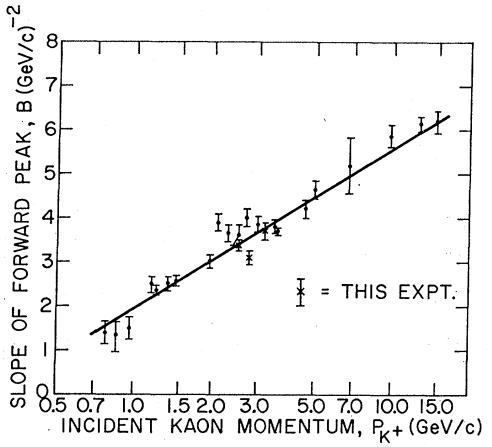

FIG. 17. Slope of the diffraction peak as a function of incident kaon momentum. The curve is a best fit to a straight line as described in the text.

best fit with $C=0$ are shown in Fig. 16 and give an excellent representation of the data to $t=-2$ (GeV/c)^2. Previously published data[12] have been fitted to Eq. (4) with $C=0$. The compilation is shown in Fig. 17, in which the existence of shrinkage is readily apparent. Another feature of Fig. 17 is the absence of any convincing structure below 3 GeV/c in contrast to the $\pi^{\pm}p$ and K^-p elastic interactions, where variations in the slope of the diffraction peak may be correlated with the positions of direct-channel resonances.[23] This absence of structure in the slope of K^+p elastic scattering is another indication of the nonexistence of a highly elastic kaon-nucleon resonant state. The curve in Fig. 17 is the result of a least-squares fit for the energy dependence of the diffraction slope to the form

$$B=2\alpha'_{\rm eff}(0)\ln(P_{K^+})+C,$$

as suggested by Regge models. [$\alpha'_{\rm eff}(0)$ is the slope of the effective trajectory exchanged.] The values obtained from this fit are $\alpha'_{\rm eff}(0)=0.79\pm0.03$ (GeV/c)$^{-2}$ and $C=1.93\pm0.06$ (GeV/c)$^{-2}$.

Morrison[24] has noted that while the K^+p and K^-p total elastic cross sections are virtually identical above $\sim$2 GeV/c as shown in Fig. 18,[25] the differential cross sections differ considerably in shape. This difference is shown in Fig. 19, where we compare our data at 2.53 GeV/c with the previously published K^-p data at 2.66 GeV/c.[26] The most noticeable features are that the K^+p data show little structure between the forward and backward peaks, whereas the K^-p data have a larger $t=0$ intercept, a steeper slope, a shoulder around $t=-0.8$ (GeV/c)^2, and a much smaller backward peak. Our data thus confirm the results from a preliminary study[27] of K^+p scattering between 2 and 3 GeV/c which indicate the absence of structure in the K^+p differential cross section near $t=-0.8$ (GeV/c)^2.

The larger K^-p intercept at $t=0$ and the smaller K^-p backward peak are qualitatively understood as a result of the larger K^-p total cross section and the absence of any positive-strangeness baryon (Z^*) which couples strongly to the elastic channel.

On the assumption that the structure near $t=-0.8$ (GeV/c)^2 in K^-p, $\pi^{\pm}p$, and $\bar{p}p$ elastic scattering is due to the annihilation scattering of quarks, one would expect similar structure in K^+p elastic scattering.[28] The absence of such a dip in K^+p scattering implies that the $\bar{\lambda}q$ amplitude is very much weaker than the nonstrange

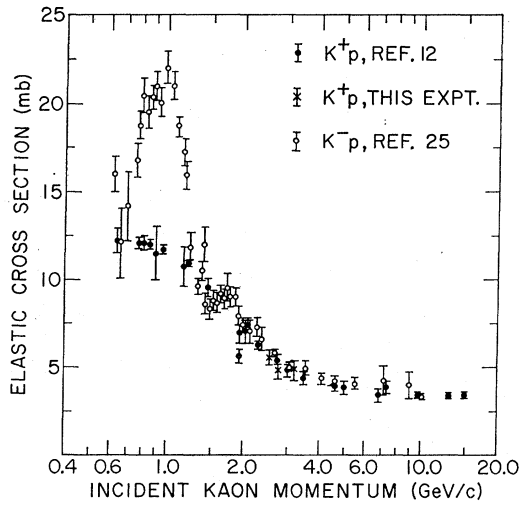

FIG. 18. Elastic cross sections for K^+p and K^-p as a function of incident kaon momentum.

[23] T. Lasinski, R. Levi-Setti, and E. Predazzi, Phys. Rev. **179**, 1426 (1969).

[24] D. R. O. Morrison, rapporteur's talk in *Proceedings of the Lund International Conference on Elementary Particles, 1969*, edited by G. von Dardel (Berlinska Boktryckeriet, Lund, Sweden, 1969).

[25] K^-p elastic scattering: (a) 0.62, 0.76, and 0.85 GeV/c—P. L. Bastien and J. P. Berge, Phys. Rev. Letters **10**, 188 (1963); (b) 0.66–1.38 GeV/c—W. R. Holley, E. F. Beall, D. Keefe, L. T. Kerth, J. J. Thresher, C. L. Wang, and W. A. Wenzel, Phys. Rev. **154**, 1273 (1967); (c) 0.78–1.23 GeV/c—B. Conforto, D. M. Harmsen, T. Lasinski, R. Levi-Setti, M. Raymund, E. Burkhardt, H. Filthuth, E. Kluge, H. Oberlack, and R. R. Ross, Nucl. Phys. **B8**, 265 (1968); (d) 1.38–2.37 GeV/c—C. Daum, F. C. Erné, J. P. Lagnaux, J. C. Sens, M. Steurer, and F. Udo, *ibid.* **B6**, 273 (1968); (e) 2.0 GeV/c—R. Crittenden, H. J. Martin, W. Kernan, L. Leipuner, A. C. Li, F. Ayer, L. Marshall, M. L. Stevenson, Phys. Rev. Letters **12**, 429 (1964); (f) 2.66 GeV/c—J. R. Ficenec, H. A. Gordon, and W. P. Trower, Phys. Rev. **175**, 1725 (1968); (g) 3.0 GeV/c—M. N. Focacci, S. Focardi, G. Giacomelli, P. Serra, M. P. Zerbetto, and L. Monari, Phys. Letters **19**, 441 (1965); (h) 3.46 GeV/c—J. Gordon, *ibid.* **21**, 117 (1966); (i) 4.07 and 5.49 GeV/c—J. Mott, R. Ammar, R. Davis, W. Kropac, A. Cooper, M. Derrick, T. Fields, L. Hyman, J. Loken, F. Schweingruber, and J. Simpson, *ibid.* **23**, 171 (1966); (j) 4.6 GeV/c—L. S. Schroeder, R. Leacock, R. L. Wagstaff, and W. J. Kernan, Phys. Rev. **176**, 1648 (1968); (k) 7.2 and 9.0 GeV/c—K. J. Foley, S. J. Lindenbaum, W. A. Love, S. Ozaki, J. J. Russell, and L. C. L. Yuan, Phys. Rev. Letters **11**, 503 (1963); (l) 10 GeV/c—Aachen-Berlin-CERN-London (I. C.)-Vienna Collaboration, Phys. Letters **24B**, 434 (1967).

[26] J. R. Ficenec *et al.*, Ref. 25(f).

[27] J. A. Danysz *et al.*, Ref. 12(k).

[28] A. I. Akhiezer and M. P. Rekalo, Yadern. Fiz. **8**, 806 (1969) [Soviet J. Nucl. Phys. **8**, 469 (1969)].

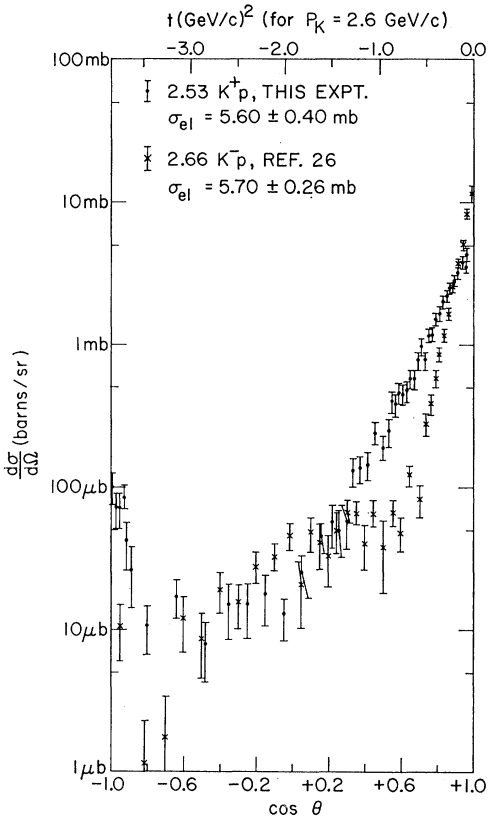

FIG. 19. Comparison of the K^+p and K^-p differential cross sections near 2.6 GeV/c.

antiquark-quark ($\bar{q}q$) amplitude. The crossover in $d\sigma/dt$ and the K^-p shoulder or second maximum are explained in the Regge model by cancellations and zeros of the contributions from the various poles (generally the ρ and ω poles) exchanged.

B. Regge Models for Kp Elastic Scattering

Since 1965 there have been several Regge-pole analyses of the forward Kp elastic and charge-exchange reactions.[8,29] The differences between these models are the assumptions made about the parametrization of the residues in the amplitudes of the exchanged trajectories.

The lowest-lying trajectories that can contribute to kaon-nucleon elastic scattering in the t channel are the Pomeranchuk trajectory P, and the P', ρ, ω, and A_2. The most recent detailed study of $K^\pm N$ reactions by Dass *et al.*[8] used not only high-energy scattering data (above $P_{\text{lab}}=5$ GeV/c), but also finite-energy sum values for $K^\pm p$ elastic-scattering amplitudes (obtained from phase-shift analyses below 1.5 GeV/c) in order to help determine the helicity-flip couplings.

[29] R. J. N. Phillips and W. Rarita, Phys. Rev. **139**, B1336 (1965); V. Singh, *ibid.* **129**, 1889 (1963); F. S. Chen-Cheung and T. Roth, *ibid.* **173**, 1768 (1968); G. Plaut, Nucl. Phys. **B9**, 306 (1969); M. L. Blackmon and G. R. Goldstein, Phys. Rev. **179**, 1480 (1968).

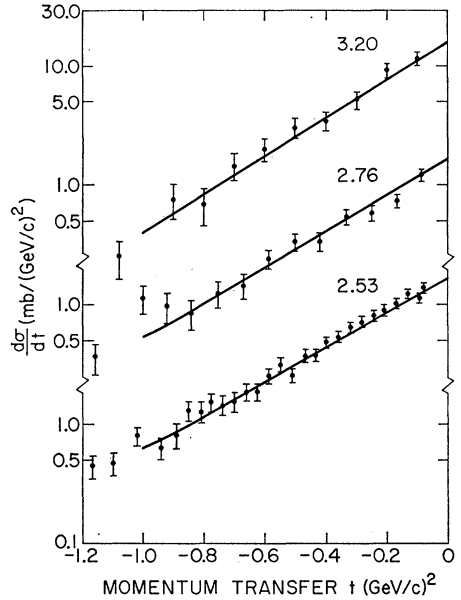

FIG. 20. Forward differential cross sections at 2.53, 2.76, and 3.20 GeV/c. The curves are an extrapolation to our energies of the Regge model calculation of Dass *et al.*, Ref. 8.

The results of extrapolating the fit of Dass *et al.* down to our momenta are shown in Fig. 20. The curves were calculated using solution (i) of Ref. 8 in which just the above five trajectories were used.[30] It may be seen that

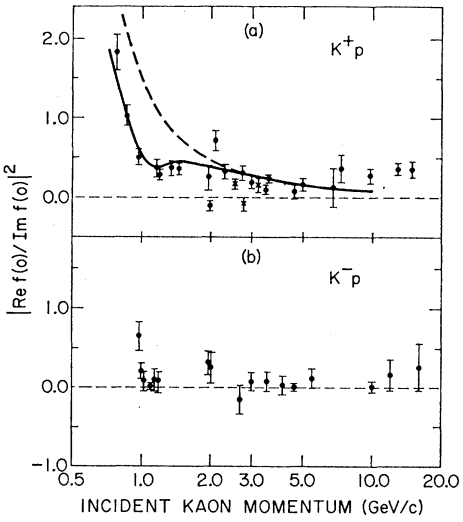

FIG. 21. Square of the ratio of the real to imaginary part of the forward scattering amplitude. The solid curve is the calculation of Carter (Ref. 31). The dashed curve is the Regge-model calculation of Dass *et al* (Ref. 8). (a) K^+p elastic scattering; (b) K^-p elastic scattering.

[30] Dass *et al.* (Ref. 8) obtained four solutions depending upon the assumptions made about an additional ω' trajectory. The four solutions appear to give almost identical results for K^+p differential cross sections. We have selected solution (i) which assumes no ω' contribution, but we do not wish to imply that the remaining solutions give worse comparisons with our data.

TABLE VII. Legendre polynomial expansion coefficients.

P_{K^+} (GeV/c)	$l_{\max}$	$(\sigma_{el}/4\pi\lambda\!\!\!^{-2})a_0$	a_1	a_2	a_3	a_4	a_5	a_6	a_7	a_8	a_9	χ^2/NDF
2.53	6	1.04±0.02	2.41±0.01	2.90±0.03	2.35±0.05	1.58±0.06	0.72±0.05	0.28±0.03				0.88
	7	1.06±0.02	2.42±0.01	2.94±0.03	2.43±0.06	1.69±0.08	0.86±0.08	0.39±0.06	0.08±0.03			0.79
	8	1.07±0.02	2.43±0.01	2.96±0.03	2.49±0.07	1.79±0.09	0.98±0.10	0.53±0.09	0.18±0.06	0.07±0.04		0.74
	9	1.06±0.03	2.43±0.01	2.95±0.04	2.47±0.07	1.75±0.10	0.93±0.12	0.48±0.12	0.12±0.10	0.03±0.07	−0.03±0.04	0.75
2.76	5	0.86±0.07	2.37±0.04	2.70±0.10	1.94±0.15	0.98±0.14	0.20±0.09					2.18
	6	0.95±0.04	2.43±0.02	2.94±0.06	2.38±0.10	1.53±0.11	0.67±0.09	0.27±0.04				0.79
	7	0.99±0.04	2.45±0.02	3.01±0.06	2.57±0.11	1.81±0.14	0.99±0.14	0.55±0.11	0.15±0.06			0.61
	8	1.00±0.04	2.46±0.02	3.03±0.06	2.60±0.12	1.87±0.16	1.07±0.18	0.62±0.15	0.22±0.12	0.06±0.08		0.62
	9	1.00±0.05	2.46±0.02	3.03±0.07	2.61±0.14	1.88±0.20	1.09±0.24	0.65±0.23	0.24±0.21	0.08±0.16	0.01±0.07	0.67
3.20	6	1.03±0.09	2.59±0.03	3.31±0.07	2.99±0.13	2.15±0.15	1.11±0.12	0.31±0.05				1.79
	7	1.17±0.06	2.60±0.01	3.45±0.05	3.37±0.10	2.64±0.13	1.68±0.13	0.96±0.14	0.36±0.08			0.70
	8	1.20±0.06	2.63±0.02	3.51±0.05	3.46±0.10	2.81±0.14	1.91±0.16	1.11±0.14	0.51±0.10	0.13±0.07		0.56
	9	1.21±0.07	2.64±0.03	3.53±0.07	3.50±0.12	2.90±0.21	2.02±0.26	1.22±0.23	0.62±0.22	0.24±0.20	0.05±0.09	0.60

the calculation is in extremely good agreement with the experimental angular distributions to $t=-1$ (GeV/c)^2 and in fact they may be extrapolated to lower energies with a fair amount of success.

Since the phase of each amplitude is specified uniquely by the signature factor for each trajectory, the over-all phase of the amplitude is given explicitly by the Regge model. In the high-energy region where the Pomeranchuk trajectory dominates [with $\alpha_P(0)=1$], the ratio of the real to imaginary part of the forward elastic amplitude becomes

$$\mathrm{Re}f(0)/\mathrm{Im}f(0)=-\cot\tfrac{1}{2}\pi\alpha_P(0)=0.$$

Experimentally this ratio may be determined by extrapolating the differential cross section to $t=0$ and making use of the optical theorem:

$$R=\left|\frac{\mathrm{Re}f(0)}{\mathrm{Im}f(0)}\right|^2=\frac{16\pi}{\sigma_T{}^2}\frac{d\sigma}{dt}(t=0)-1,$$

where σ_T is the total cross section.[1] The results of the present experiment, $R=0.16\pm0.06$, -0.08 ± 0.07, and 0.17 ± 0.11 at 2.53, 2.76, and 3.20 GeV/c, respectively, are shown in Fig. 21(a) along with those from previously reported data.[12] The dashed curve is the result of the Regge model of Dass *et al.*[8] The solid curve is a calculation by Carter[31] using forward dispersion relations and $K^{\pm}N$ total cross-section data. The interesting feature of this figure is the apparent increase in the real amplitude above 5 GeV/c in contrast to the Regge-model fit of Dass *et al.* The results of Carter also tend to zero at high energy because the dispersion integral above 5 GeV/c uses a Regge extrapolation to higher energies.

If this increase in the real part of the forward amplitude is confirmed, it would be interesting to speculate on an explanation. Perhaps, as Eden suggests,[32] it is related to the fact that the latest Serpukhov data indicate that the $K^{\pm}p$ total cross sections are not asympotically equal.[33] This might indicate that the real part of the $K^{\pm}p$ forward amplitudes should increase logarithmically with energy.[32] A measure of the real part at very high energy would therefore be of great interest. We note that the situation in K^-p elastic scattering [Fig. 21(b)] at high energy is even more uncertain.[25]

V. PARTIAL-WAVE ANALYSIS

A. Legendre Polynomial Expansion

As a preliminary step in performing a phase-shift analysis on the complete angular distributions reported in this paper, we have fitted the differential cross sections with a Legendre polynomial expansion of the form

$$\frac{d\sigma}{d\Omega}(s,\theta)=\lambda\!\!\!^{-2}\sum_{l=0}^{\infty}\beta_l(s)P_l(\cos\theta). \tag{5}$$

One may then study the coefficients $a_l(s)=\beta_l(s)/\beta_0(s)$ as a function of incident momentum. The normalization is such that $\sigma_{el}=4\pi\lambda\!\!\!^{-2}\beta_0$. The highest-order polynomial required at each momentum and denoted by $l_{\max}$ was determined on the basis of three nonindependent criteria. $l_{\max}$ was selected to be the order for which

(a) the first minimum in χ^2/NDF occurred, where NDF is the number of degrees of freedom, (b) the quantities $a_l(0\leq l\leq l_{\max})$ did not change significantly upon trying to fit to order $l=l_{\max}+1$, or (c) the quantity $a_{l_{max}+1}$ was consistent with zero when the fit to order $l_{\max}+1$ was tried.

These criteria are illustrated in Table VII and the curves on Figs. 7–9 are the results of the best fit to Eq. (5) using the following values of $l_{\max}$:

$l_{\max}$	Momentum (GeV/c)
8	2.53
7	2.76
8	3.20

[31] A. A. Carter, Cavendish Laboratory Report No. HEP 68-10, 1968 (unpublished).

[32] R. J. Eden, Phys. Rev. D **2**, 529 (1970).

[33] J. V. Allaby, Yu. B. Bushnin, S. P. Denisov, A. N. Diddens, R. W. Dobinson, S. V. Donskov, G. Giacomelli, Yu. P. Gorin, A. Klovning, A. I. Petrukin, Yu. D. Prokoshkin, R. S. Shuvalov, C. A. Stahlbrant, and D. A. Stoyanova, Phys. Letters **30B**, 500 (1969).

An examination of the coefficients in Table VII indicates that at 2.76 and 3.20 GeV/c we observe a monotonic dependence of a_l with an increasing order of the polynomial expansion. We shall limit our phase-shift analysis, therefore, to the data at 2.53 GeV/c.

B. Phase-Shift Analysis

As a further study of the possible existence of KN resonances, an energy-independent phase-shift analysis has been performed on the complete differential cross section at 2.53 GeV/c. The expressions used are those of Roper *et al.*[34] In addition to the measured cross section, the polarization data of Andersson *et al.* at 2.48 GeV/c were also used.[35] Using 100 different starting points and the minimizing program MINFUN,[36] we obtained five regions of minima which are shown in Fig. 22 as the shaded areas on an Argand diagram. While no quantitative continuation from lower-energy analyses[37] is feasible at the present time, the results obtained here are not inconsistent with possible extrapolations from 2 GeV/c. In particular, several of the solutions would appear to be consistent with continuations of a counterclockwise semicircle observed in the $P_{3/2}$ wave by phase-shift analyses below 2 GeV/c.

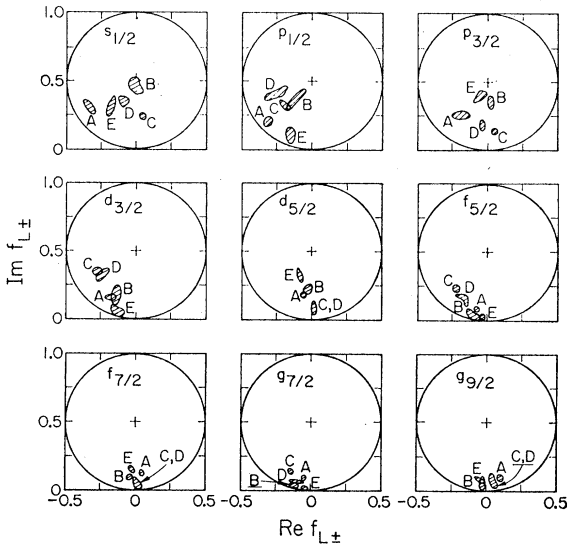

FIG. 22. Argand diagrams for the partial wave amplitudes at 2.5 GeV/c. The shaded areas indicate the regions in which the solutions tended to occur.

VI. SUMMARY

The K^+p elastic-scattering distributions obtained in this and other experiments indicate that near the backward direction there appears to be some anomalous structure between 2 and 3 GeV/c. Our results indicate that expressions based on EXD hyperon exchange Regge amplitudes that parametrize both low- and high-energy K^+p elastic-scattering data are unable to reproduce the backward data between 2 and 3 GeV/c. No such discrepancy between Regge models and experiment has been found in our forward scattering data which confirm the absence of any structure in $d\sigma/dt$ near $t=-0.8$ $(\mathrm{GeV}/c)^2$.

The results from this experiment which was designed to study the K^+p total cross-section enhancement at 2.75 GeV/c would appear to be inconclusive as far as evidence for or against the existence of any Z^* resonances is concerned, although the structure observed in the backward direction would appear to be suggestive. Our partial-wave analysis at 2.5 GeV/c is in general qualitative agreement with continuations of previous lower-energy analyses.

ACKNOWLEDGMENTS

We would like to acknowledge the help of Dr. L. Voyvodic, Dr. F. Schweingruber, and the Argonne National Laboratory 30-in. bubble chamber crew during the experimental exposure. We would also like to thank Professor E. L. Goldwasser for his participation during the initial stages of this experiment. Finally, we would like to thank the scanners and measurers at the University of Illinois for their conscientious efforts during all phases of this experiment.

[34] L. D. Roper, R. M. Wright, and B. T. Feld, Phys. Rev. **138**, B190 (1965).

[35] S. Andersson, C. Daum, F. C. Erné, J. P. Lagnaux, J. C. Sens, and F. Udo, Phys. Letters **28B**, 611 (1969).

[36] W. Humphrey and B. Cottrell, LRL Physics Notes, Memo No. P-6 (Rev.) (unpublished).

[37] S. Andersson, C. Daum, F. C. Erné, J. P. Lagnaux, J. C. Sens, F. Udo, and F. Wagner, Phys. Letters **30B**, 56 (1969); in *Proceedings of the Lund International Conference on Elementary Particles, 1969*, edited by G. von Dardell (Berlinska, Boktryckeriet, Lund, Sweden, 1969). J. G. Asbury, J. D. Dowell, S. Kato, D. Lundquist, T. B. Novey, A. Yokosawa, B. Barnett, P. F. M. Koehler, and P. Steinberg, Phys. Rev. Letters **23**, 194 (1969); G. A. Rebka, Jr., J. Rothberg, A. Etkin, P. Glodis, J. Greenberg, V. W. Hughes, K. Kondo, D. C. Lu, S. Mori, and P. A. Thompson, *ibid.* **24**, 160 (1970); S. Kato, P. Koehler, T. Novey, A. Yokosawa, and G. Burleson, *ibid.* **24**, 615 (1970).